ChemComm

Cite this: *Chem. Commun.*, 2012, **48**, 7289–7291

www.rsc.org/chemcomm

COMMUNICATION

Iron phosphate microflowers as peroxidase mimic and superoxide dismutase mimic for biocatalysis and biosensing†

Wei Wang,* Xiangpeng Jiang and Kezheng Chen*

Received 4th April 2012, Accepted 23rd May 2012
DOI: 10.1039/c2cc32429f

Novel iron phosphates microflowers which show SOD-like and peroxidase-like mimic activities were prepared, suggesting potential applications as a biocatalyst and a biosensor for H_2O_2.

Peroxidase and superoxide dismutase (SOD) are both enzymes that act as natural antioxidants to defend oxidative stress related to reactive oxygen species (ROS) such as $O_2^{\bullet -}$, $OH^{\bullet}$ and H_2O_2. Peroxidases are a large family of enzymes that typically catalyze oxidation of many organic substrates to reduce their toxicity. For instance, peroxidase can activate the oxidation, by hydrogen peroxide, of various metabolites and toxins. It does so according to the reaction in eqn (1). SODs are a class of enzymes that catalyze the dismutation of $O_2^{\bullet -}$ into O_2 and H_2O_2, which may be written as the reaction in eqn (2).

$$H_2O_2 + H_2R \rightarrow 2H_2O + R \quad (1)$$

$$2O_2^{\bullet -} + 2H^+ \rightarrow H_2O_2 + O_2 \quad (2)$$

Although the exact mechanism of these reactions is not very clear, peroxidase and SOD are regarded as antioxidants by protecting cells against damage from ROS, which may be important in Parkinson's and Alzheimer's disease, cardiovascular disease and tumor development.[1]

Being protein-based macromolecules, natural enzymes have disadvantages in that they are unstable against denaturation or protease digestion and hence their preparation, purification and storage are usually time-consuming and expensive. Recent progress in pushing these limits with enzyme mimics remains outweighed by substantial trade-offs in enzyme-like activities, physical stability, large-scale feasibility, and/or difficulty and expense of fabrication. Many artificial organic molecules including hemin,[2a] porphyrin,[2b] molecularly imprinted hydrogels[2c] and DNAzyme[2d] have been developed as peroxidase mimics.

Since the surprising discovery that Fe_3O_4 nanoparticles possess intrinsic peroxidase-like activity,[3a] nanomaterial-based enzyme mimics have garnered increasing interest due to their favorable reactivity, easy fabrication and low-cost storage superior to organic molecules. Subsequently, FeS nanosheets,[3b] CeO_2 nanoparticles,[3c] carbon nanotubes,[3d] graphene oxide,[3e] Au nanoparticles,[3f,g] $BiFeO_3$ nanoparticles[3h] and $CoFe_2O_4$ magnetic nanoparticles[3i] were found to have peroxidase, oxidase or SOD mimetic activities.

Iron phosphates (FePOs), are a well-known catalyst that selectively catalyzes the oxidative dehydrogenation of saturated carboxylic acids[4] and are of research interest for many applications in catalysis. In the present work, we report the facile preparation of iron phosphate microflowers that show peroxidase-like and SOD-like activities. The reaction between H_2O_2 and 3,3′,5,5′-tetramethylbenzidine (TMB) was found to be catalyzed by the prepared FePOs microflowers, indicating the peroxidase-like activity of the products. Furthermore the inhibition of oxidation of pyrogallol by the prepared microflowers suggested that they can also serve as an SOD mimic.

The XRD pattern of the products (Fig. S1, ESI†) shows the presence of two phases of iron-phosphate compositions. The peaks marked by rectangles can be indexed to $Na_{4.55}Fe(PO_4)_2H_{0.45}O$ (JCPDS card No. 52-1393) and those marked by asterisks can be indexed as the $FeH_3P_2O_8{}^{\bullet}H_2O$, which is in good agreement with the values in the standard card (JCPDS card No. 46-0197). For $FeH_3P_2O_8{}^{\bullet}H_2O$ compound, the redox state of the Fe element is +3 whereas it is +2 for $Na_{4.55}Fe(PO_4)_2H_{0.45}O$. Consequently the products are regarded to have a mixed valence Fe element, which may be further identified by the mixed color of the products (inset of Fig. S1†), *i.e.*, yellow-greenish grey accompanied with brown.

SEM image in Fig. 1 shows that the products have flower-like morphology assembled by straight 1-dimensional nanostructures with a diameter of 80–100 nm and length up to several micrometers.

The redox reaction between TMB and H_2O_2 was carried out to study the peroxidase mimetic activity of the FePOs

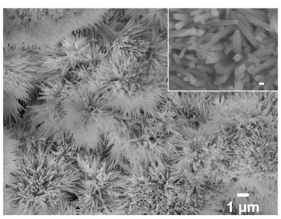

Fig. 1 SEM image of FePOs microflowers. The inset is high-magnification SEM image with a scale bar of 100 nm.

Lab of Functional and Biomedical Nanomaterials, College of Materials Science and Engineering, Qingdao University of Science and Technology, Qingdao, 266042, China. E-mail: wangwei@qust.edu.cn, kchen@qust.edu.cn; Fax: +86-532-84022814

† Electronic supplementary information (ESI) available: Experimental section, Fig. S1–S7 and Table S1 and S2. See DOI: 10.1039/c2cc32429f

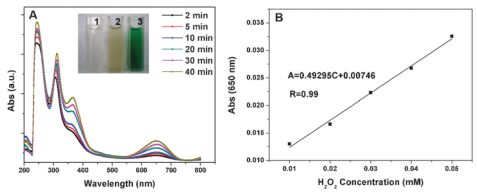

Fig. 2 (A) Typical UV-Vis spectra of TMB-H_2O_2-FePOs reaction system in timescan mode (2 mL of 2.5 mM TMB, 25 μL of 10 mM H_2O_2, 50 μL of 400 μg ml^{-1} FePOs, 425 μL of ultrapure water). (B) Linear calibration plot between the absorbance at 650 nm and concentration of H_2O_2. The inset of (A) shows different colors of (1) TMB-H_2O_2 mixed solution without FePOs microflowers, (2) FePOs microflowers without TMB and (3) TMB-H_2O_2 mixed solution with FePOs microflowers.

microflowers. In solution, colorless TMB forms a blue product when allowed to react with catalase or peroxidase enzymes. The resulting color change can be read on a spectrophotometer at a wavelength of 370 or 650 nm.

UV-Vis spectra (Fig. 2A) monitoring the reaction system containing TMB, H_2O_2 and FePOs microflowers clearly shows an increase of absorbance at 370 and 650 nm, and the blue color correspondingly developed (inset of Fig. 2A), indicating the peroxidase-like activity of the FePOs microflowers. Fig. 2B shows the calibration curve of the absorbance at 650 nm against H_2O_2 concentration. The curve was linear in a range from 1×10^{-5} M to 5×10^{-5} M with a detection limit of 10 nM, indicating a potential novel strategy to detect H_2O_2 concentration. Such enzyme mimetic capability may be ascribed to the reversible switching of the Fe^{3+}/Fe^{2+} redox couple present in the FePOs products, which occurs in the reaction centers of a number of peroxidase enzymes[5] and some iron-based compounds such as Fe_3O_4 nanoparticles,[3a] FeS nanosheets[3b] and Prussian blue.[6]

The steady-state kinetic assays were carried out at room temperature in TMB-H_2O_2-FePOs reaction system (for detailed process see ESI†). Catalytic parameters were determined by fitting the absorbance data to the Michaelis–Menten equation (eqn (3)).

$$dv = \frac{v_{max}[S]}{K_m + [S]} \quad (3)$$

In this equation, v is the rate of conversion, v_{max} is the maximum rate of conversion, $[S]$ is the substrate concentration, and K_m is the Michaelis constant.

Initial absorbance against time plots shown in Fig. S3.† indicate typical Michaelis–Menten kinetics displayed by the TMB-H_2O_2 reactions catalyzed by the FePOs microflowers. The slopes of these plots are calculated as initial reaction rates as different concentrations of substrate. By plotting reaction rate against concentration (Fig. 3), and using nonlinear regression of the Michaelis–Menten equation, the catalytic parameters of K_m and v_{max} were obtained (Table S1†).

The K_m value of the FePOs microflowers with H_2O_2 as the substrate was 0.317 mM, which is lower than that reported for horseradish peroxidase (HRP, 3.7 mM), indicating that the FePOs microflowers have a higher affinity for H_2O_2 than HRP. Compared with that of HRP, the K_m value of FePOs microflowers with TMB as the substrate is significantly higher.

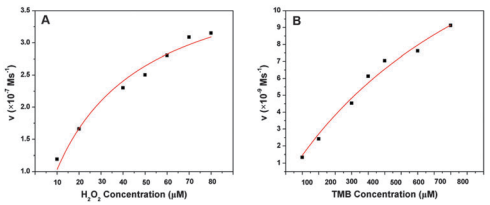

Fig. 3 Kinetic analysis for FePOs microflowers with (A) H_2O_2 and (B) TMB as substrates, respectively. A steady-state catalysis rate was calculated from the initial slopes of absorbance *vs.* time curves.

Although the exact molar mass of FePOs microflowers is unknown, the K_{cat}/K_m value of FePOs microflowers with H_2O_2 as substrate is calculated to be 10 to 100 times of that for HRP. This enhancement was consistent with the lower K_m value of FePOs taking H_2O_2 as a substrate. However, the K_{cat}/K_m value of FePOs microflowers with TMB as substrate was significantly smaller than that for HRP, corresponding to the larger K_m value of FePOs with TMB as substrate. These results indicate that FePOs microflowers exhibit greater catalytic efficiency than HRP considering H_2O_2 as a substrate but lower efficiency for TMB.

The SOD mimetic activity of FePOs microflowers was assayed spectrophotometrically by measuring the inhibition of auto-oxidation of pyrogallol, according to the method of S. Marklund and G. Marklund.[7] Pyrogallol can be auto-oxidized under alkaline condition and the auto-oxidation product has an absorption peak at 320 nm, whereas the process may be greatly inhibited by an SOD.

Fig. S5† shows the UV-Vis spectra of pyrogallol in timescan mode at 320 nm with and without the prepared FePOs microflowers upon reaction for 15 min. The absorption changes against time plots (Fig. 4A) clearly demonstrated the inhibition effect on oxidation of pyrogallol by the FePOs products, thus indicated the SOD activity of the FePOs. As in the peroxidase mimetic capability, the expected conversion of Fe^{2+}/Fe^{3+} is also implicated in the SOD mimetic capability of FePOs. As shown in the color change images (inset of Fig. 4B), the pyrogallol solution in 0.1 M Tris-HCl finally became yellow-brown after auto-oxidation of pyrogallol (bottle 3) but turned purple in the presence of the FePOs microflowers (bottle 2). Since Fe^{3+} ions are well-known to form purple

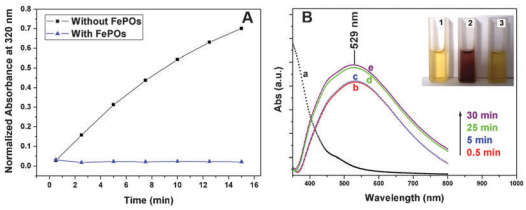

Fig. 4 (A) Time-dependent absorbance changes at 320 nm of pyrogallol solution in 0.1 M Tris-HCl buffer with and without FePOs microflowers (400 μg ml^{-1}), (B) UV-vis spectra of (a) FePOs microflowers in 0.1 M Tris-HCl buffer without pyrogallol and (b–e) UV-vis absorption-time course curves of pyrogallol solution in 0.1 M Tris-HCl with FePOs microflowers. The inset of (B) shows different colors of (1) FePOs microflowers in 0.1 M Tris-HCl, (2) pyrogallol solution in 0.1 M Tris-HCl with FePOs microflowers and (3) without FePOs microflowers.

complexes with polyphenol ligands, the SOD mimic mechanism of the FePOs may probably follow the eqn (4).

$$Fe^{2+} + O_2^{\bullet -} + 2H^+ \rightarrow H_2O_2\ Fe^{3+} \qquad (4)$$

In this mechanism, Fe^{2+} ions are ascribed as reactive centers which capture $O_2^{\bullet -}$ and transform into Fe^{3+} ions. The formed Fe^{3+} ions then complex with polyphenol ligands to give a purple solution. The fact that an absorption band with λ_{max} of 529 nm in UV-Vis spectrum (curve b, Fig. 4B) was immediately found after the addition of FePOs further identifies the change in redox state of Fe ions. Previous research reported that at slightly acidic pH (5–6.5) the iron(III) polyphenol complexes displayed λ_{max} in the ranges of 542–561 nm for gallates due to the ligand-to-metal charge transfer (LMCT) bands.[8] The blue shift of λ_{max} compared with literature values may be due to the slightly larger pH ($\sim$6.8)[8b] in present work. Moreover the absorption of this band increased over time (curve c–e, Fig. 4B), suggesting that more and more Fe^{2+} transform into Fe^{3+}. The conclusion that Fe^{2+} ions act as reactive centers is in consistent with some polyphenol compounds and their complexes with Fe^{2+} which are reported to react with superoxide ($O_2^{\bullet -}$) and show SOD-like behavior.[8a,9]

The catalytic activity of the FePOs microflowers was found to dependent on pH and temperature. Data shown in Fig. S6† demonstrate that being other conditions equal the UV-Vis absorption at 650 nm increased most rapidly and reached the highest level at pH 4.5 and 30 °C for the TMB-H_2O_2 reaction catalyzed by the FePOs sample, consistent with the deepest blue at pH 4.5 and 30 °C shown in insets of Fig. S6.† Consequently, optimal pH and temperature were approximately pH 4.5 and 30 °C for peroxidase-like activity of the FePOs microflowers. Data in Fig. S7† indicate that pyrogallol-oxidation reaction can be inhibited by the FePOs sample all over the pH range of 7.5–12 and temperature range of 20–70 °C, suggesting that the SOD-like activity of FePOs was not significantly influenced by the pH and temperature. We didn't investigate the effect of pH on the SOD-like activity of FePOs for the pH lower than 7.5, since pyrogallol autoxidation reaction usually occurs in the alkaline condition and we didn't observe detectable change of 320 nm absorption when the pH value was lower than 7.

In summary, FePOs microflowers that exhibit both peroxidase and SOD mimetic activities were fabricated *via* a facile method. Expected conversion of Fe^{2+}/Fe^{3+} is implicated in the peroxidase and SOD mimetic capabilities. The oxidation of peroxidase substrate TMB with H_2O_2 catalyzed by FePOs microflowers was realized and provided a colorimetric assay for H_2O_2. It was thoroughly observed that the peroxidase activity of the FePOs microflowers showed typical Michaelis–Menten kinetics exhibiting higher efficiency with H_2O_2 as a substrate compared to HRP. The inhibition effect on oxidation of pyrogallol accomplished by the FePOs microflowers indicated the SOD activity of the FePOs. Further investigations demonstrated that Fe^{2+} ions act as reactive centers to react with $O_2^{\bullet -}$ and show SOD-like behavior. Inspired by the facial fabrication, cost effectiveness and dual-enzyme mimetic activities of peroxidase-like and SOD-like behaviors, we expect that our FePOs microflowers will find potential applications as a biocatalyst or an antioxidant for clinical trials to fight ROS related diseases.

This work was financially supported by National Natural Science Foundation of China (Grant No. 50902077, 51072087), Specialized Research Fund for the Doctoral Program of Higher Education (Grant No. 20113719110001) and Development Program in Science and Technology of Qingdao (Grant No. JK2011-8).

Notes and references

1 R. S. Williams, S. A. Johnston, M. Riedy, M. J. DeVit, S. G. McElligott and J. C. Sanford, *Proc. Natl. Acad. Sci. U. S. A.*, 1991, **88**, 2726.

2 (*a*) Q. Wang, Z. Yang, X. Zhang, X. Xiao, C. K. Chang and B. Xu, *Angew. Chem., Int. Ed.*, 2007, **46**, 4285; (*b*) M. Sono, M. P. Roach, E. D. Coulter and J. H. Dawson, *Chem. Rev.*, 1996, **96**, 2841; (*c*) G. Pelossof, R. Tel-Vered, J. Elbaz and I. Willner, *Anal. Chem.*, 2010, **82**, 4396.

3 (*a*) L. Gao, J. Zhuang, L. Nie, J. Zhang, Y. Zhang, N. Gu, T. Wang, J. Feng, D. Yang, S. Perrett and X. Yan, *Nat. Nanotechnol.*, 2007, **2**, 577; (*b*) Z. H. Dai, S. H. Liu, J. C. Bao and H. X. Ju, *Chem.–Eur. J.*, 2009, **15**, 4321; (*c*) T. Pirmohamed, J. M. Dowding, S. Singh, B. Wasserman, E. Heckert, A. S. Karakoti, J. E. King, S. Seal and W. T. Self, *Chem. Commun.*, 2010, **46**, 2736; (*d*) Y. J. Song, X. H. Wang, C. Zhao, K. G. Qu, J. S. Ren and X. G. Qu, *Chem.–Eur. J.*, 2010, **16**, 3617; (*e*) Y. J. Song, K. G. Qu, C. Zhao, J. S. Ren and X. G. Qu, *Adv. Mater.*, 2010, **22**, 2206; (*f*) Y. Jv, B. X. Li and R. Cao, *Chem. Commun.*, 2010, **46**, 8017; (*g*) Y. J. Long, Y. F. Li, Y. Liu, J. J. Zheng, J. Tang and C. Z. Huang, *Chem. Commun.*, 2011, **47**, 11939; (*h*) W. Luo, Y.-S. Li, J. Yuan, L. H. Zhu, Z. D. Liu, H. Q. Tang and S. S. Liu, *Talanta*, 2010, **81**, 901; (*i*) W. B. Shi, X. D. Zhang, S. H. He and Y. M. Huang, *Chem. Commun.*, 2011, **47**, 10785.

4 (*a*) P. Bonnet, J. M. M. Millet, C. Leclercq and J. C. Vedrine, *J. Catal.*, 1996, **158**, 128; (*b*) M. Ai, E. Muneyama, A. Kunishige and K. J. Ohdan, *J. Catal.*, 1993, **144**, 632; (*c*) K.-H. Lii, Y.-F. Huang, V. Zima, C.-Y. Huang, H.-M. Lin, Y.-C. Jiang, F.-L. Liao and S.-L. Wang, *Chem. Mater.*, 1998, **10**, 2599; (*d*) D. H. Yu, C. Wu, Y. Kong, N. H. Xue, X. F. Guo and W. P. Ding, *J. Phys. Chem. C*, 2007, **111**, 14394.

5 (*a*) S. Q. Liu and H. X. Ju, *Anal. Biochem.*, 2002, **307**, 110; (*b*) H. X. Ju, S. Q. Liu, B. X. Ge, F. Lisdat and F. W. Scheller, *Electroanalysis*, 2002, **14**, 141; (*c*) Y. M. Yan, W. Zheng, M. N. Zhang, L. Wang, L. Su and L. Q. Mao, *Langmuir*, 2005, **21**, 6560.

6 (*a*) A. Karyakin, E. Puganova, I. Budashov, I. Kurochkin, E. Karyakina, V. Levchenko, V. Matveyenko and S. Varfolomeyev, *Anal. Chem.*, 2004, **76**, 474; (*b*) A. Karyakin, E. Karyakina and L. Gorton, *Anal. Chem.*, 2000, **72**, 1720; (*c*) A. Karyakin, O. Guitelmaker and E. Karyakina, *Anal. Chem.*, 1995, **67**, 2419; (*d*) A. Karyakin and E. Karyakina, *Sens. Actuators, B*, 1999, **57**, 268; (*e*) P. A. Fiorito, V. R. Goncales, E. A. Ponzio and S. I. Cordoba de Torresi, *Chem. Commun.*, 2005, 366; (*f*) J. Li, J. D. Qiu, J. J. Xu, H. Y. Chen and X. H. Xia, *Adv. Funct. Mater.*, 2007, **17**, 1574; (*g*) E. A. Puganova and A. A. Karyakin, *Sens. Actuators, B*, 2005, **109**, 167; (*h*) X. Q. Zhang, S.-W. Y. Gong, Y. Zhang, T. Yang, C.- Yu, Wang and N. Gu, *J. Mater. Chem.*, 2010, **20**, 5110.

7 S. Marklund and G. Marklund, *Eur. J. Biochem.*, 1974, **47**, 469.

8 (*a*) N. R. Perron and J. L. Brumaghim, *Cell Biochem. Biophys.*, 2009, **53**, 75; (*b*) N. R. Perron, J. N. Hodges, M. Jenkins and J. L. Brumaghim, *Inorg. Chem.*, 2008, **47**, 6153.

9 (*a*) K. Furuno, T. Akasako and N. Sugihara, *Biol. Pharm. Bull.*, 2002, **25**, 19; (*b*) R. F. V. De Souza, E. M. Sussuchi and W. F. De Giovani, *Synth. React. Inorg. Met.-Org. Chem.*, 2003, **33**, 1125; (*c*) J. R. Reddan, F. J. Giblin, M. Sevilla, V. Padgaonkar, D. C. Dziedzic, V. R. Leverenz, I. C. Misra, J. S. Chang and J. T. Pena, *Exp. Eye Res.*, 2003, **76**, 49; (*d*) V. A. Kostyuk, A. I. Potapovich, E. N. Strigunova, T. V. Kostyuk and I. B. Afanas'ev, *Arch. Biochem. Biophys.*, 2004, **428**, 204; (*e*) I. B. Afanas'ev, E. A. Ostrakhovitch, E. V. Mikhal'chik, G. A. Ibragimova and L. G. Korkina, *Biochem. Pharmacol.*, 2001, **61**, 677.